JACS
JOURNAL OF THE AMERICAN CHEMICAL SOCIETY
Article
pubs.acs.org/JACS

A Bimetallic Nickel–Gallium Complex Catalyzes CO_2 Hydrogenation via the Intermediacy of an Anionic d^{10} Nickel Hydride

Ryan C. Cammarota,[†] Matthew V. Vollmer,[†] Jing Xie,[†,‡] Jingyun Ye,[†,‡] John C. Linehan,[§] Samantha A. Burgess,[§] Aaron M. Appel,[§] Laura Gagliardi,[†,‡] and Connie C. Lu*[,†]

[†]Department of Chemistry, University of Minnesota, 207 Pleasant Street SE, Minneapolis, Minnesota 55455, United States
[‡]Supercomputing Institute and Chemical Theory Center, University of Minnesota, Minneapolis, Minnesota 55455, United States
[§]Pacific Northwest National Laboratory, P.O. Box 999, MS K2-57, Richland, Washington 99352, United States

Supporting Information

ABSTRACT: Large-scale CO_2 hydrogenation could offer a renewable stream of industrially important C_1 chemicals while reducing CO_2 emissions. Critical to this opportunity is the requirement for inexpensive catalysts based on earth-abundant metals instead of precious metals. We report a nickel–gallium complex featuring a Ni(0)→Ga(III) bond that shows remarkable catalytic activity for hydrogenating CO_2 to formate at ambient temperature (3150 turnovers, turnover frequency = 9700 h^{-1}), compared with prior homogeneous Ni-centered catalysts. The Lewis acidic Ga(III) ion plays a pivotal role in stabilizing catalytic intermediates, including a rare anionic d^{10} Ni hydride. Structural and *in situ* characterization of this reactive intermediate support a terminal Ni–H moiety, for which the thermodynamic hydride donor strength rivals those of precious metal hydrides. Collectively, our experimental and computational results demonstrate that modulating a transition metal center via a direct interaction with a Lewis acidic support can be a powerful strategy for promoting new reactivity paradigms in base-metal catalysis.

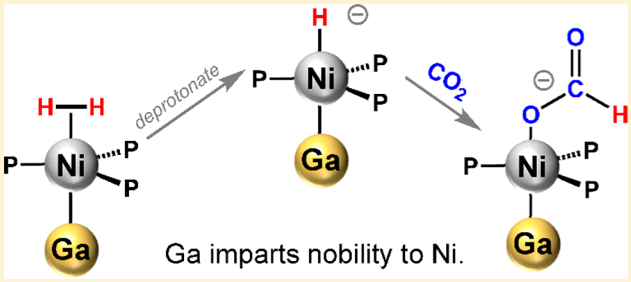

INTRODUCTION

Efficient recycling of CO_2 to industrial chemicals and liquid fuels, such as formic acid or methanol, could generate value-added products from an abundant C_1 feedstock while alleviating adverse effects associated with rising CO_2 levels. Although a CO_2-to-fuel scheme would require efficient CO_2 capture and sustainable H_2 production,[1] we focus on the singularly formidable challenge of developing base-metal catalysts for selective CO_2 hydrogenation under mild conditions.[2−5] CO_2 hydrogenation to methanol remains a daunting task; the few known molecular catalysts rely almost exclusively on precious metals (Ru, Ir),[6−11] with only a single instance of a base-metal (Co) catalyst.[12] Furthermore, base-metal catalysts remain uncommon for the hydrogenation of CO_2 to formate.[13−17] In the past few years, impressive catalytic performance has been achieved using phosphine-ligated Fe and Co catalysts, which generate formate with turnover numbers (TONs) from 9000 to 59 000 with high turnover frequencies (TOFs).[18−20]

Despite the aforementioned recent advances with Fe and Co catalysts, the progress of Ni-based systems for CO_2 hydrogenation has been limited.[21−23] The first homogeneous Ni catalyst was reported over 40 years ago: $Ni(dppe)_2$, where dppe = bis(diphenylphosphino)ethane, produced formate from H_2 and CO_2, albeit with poor activity (TON = 7, TOF = 0.35 h^{-1}).[21] Recently, a water-soluble Ni bis(diphosphine) catalyst was found to mediate the H_2/CO_2-to-formate reaction in aqueous solution using $NaHCO_3$ as the base, but the activity remained low (TOF of 0.40(5) h^{-1} at 80 °C and 34 atm of H_2/CO_2).[23] In a related work, a Ni PCP-pincer catalyst generated formate from H_2 and $NaHCO_3$ with a comparatively impressive TON of 3000 at 150 °C and 54 atm; however, the catalyst was inactive when $NaHCO_3$ was replaced with CO_2.[24]

The dearth of Ni catalysts for CO_2 hydrogenation stems from several inherent limitations. Ni, being more electronegative than Fe and Co, has a lower propensity for activating H_2 to generate Ni–H,[25] and once generated, the resulting Ni–H species are typically weak hydride donors. Furthermore, Ni–H complexes which are potent enough hydride donors to react with CO_2 tend to form strong Ni–O bonds, which prevent formate liberation.[26] This lack of strong hydride donors is illustrated by the fact that even for the most hydridic Ni–H reported,[26] $[HNi(dmpe)_2]^+$ (dmpe = bis(dimethylphosphino)ethane) with a thermodynamic hydricity ($\Delta G^\circ_{H^-}$) of 49.9 kcal/mol in CH_3CN, outer-sphere hydride transfer to CO_2 to generate free formate (cf. $\Delta G^\circ_{H^-}$ = 44 kcal/mol) is thermodynamically unfavorable by ∼6 kcal/mol in CH_3CN.[27,28] However, it should be noted that there are several examples of Ni–H complexes that are sufficiently

Received: July 27, 2017
Published: September 12, 2017

DOI: 10.1021/jacs.7b07911
J. Am. Chem. Soc. 2017, 139, 14244−14250

hydridic to react with CO_2 to form η^1-O formate adducts of Ni.[26] In these cases, the more salient issue that precludes catalytic CO_2 hydrogenation is the formation of strong Ni−O bonds, which impede formate release and thus prevent catalytic turnover. Catalytic liberation of CO_2 reduction products in these systems can be accomplished in some cases using stoichiometric boranes or silanes to form strong B−O or Si−O bonds, which permit Ni−O bond cleavage and drive catalytic turnover. For example, Ni POCOP-pincer complexes can rapidly insert CO_2 into Ni−H bonds and further reduce CO_2 to methoxides using stoichiometric borane.[29] The requirement of B−H or Si−H reductants to drive catalysis, however, is a drawback in that the overall transformations lack atom economy.[29,30]

Circumventing the inherent limitations of Ni in CO_2 hydrogenation would involve stabilizing Ni−H in more reduced charge states and/or lower Ni oxidation states,[31,32] while still allowing the regeneration of Ni−H from H_2 and base.[33,34] A highly reduced Ni center could potentially allow for both facile hydride transfer from a Ni−H species to CO_2, along with a decreased propensity for undesirably strong formate binding in the subsequent step. Specifically, our strategy involves the incorporation of a Lewis acidic Ga(III) metalloligand, which acts as a σ-acceptor toward Ni in NiGaL (**1**).[35−39] We have previously shown that positioning the supporting Ga(III) ion directly *trans* to the substrate binding site at Ni allows for H_2 binding to form a nonclassical H_2 adduct, (η^2-H_2)NiGaL, under 1 atm of H_2 (Figure 1).[39,40] In this combined experimental and

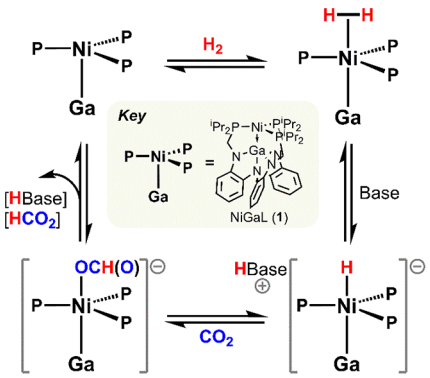

Figure 1. General catalytic scheme for H_2/CO_2 to formate by NiGaL (**1**). A key step is the base-assisted H_2 heterolysis of (η^2-H_2)NiGaL to form the anionic Ni hydride intermediate, [HNiGaL]$^-$.

theoretical study, we show that the Ga(III) support plays a vital role in stabilizing a d^{10} terminal Ni−H species which is strongly hydridic, with an estimated $\Delta G^\circ_{H^-}$ value of ∼31 kcal/mol in CH_3CN. Based on this low $\Delta G^\circ_{H^-}$ value, the hydride donor strength of the unusual anionic Ni−H species rivals those of precious metal hydrides, allowing for spontaneous reaction with CO_2 to generate and release formate.[41] Taken together, the supporting Ga(III) ion modulates the properties of Ni so as to promote H_2 heterolysis and stabilize a highly reactive Ni−H species, affording a Ni catalyst capable of mediating efficient CO_2 hydrogenation to formate at room temperature.

■ RESULTS AND DISCUSSION

Catalysis. Under ambient conditions (1 atm 1:1 H_2/CO_2, 293 K), complex **1** catalyzes CO_2 hydrogenation to formate in 91% yield (0.36 mol % catalyst loading; Table 1, entry 1). A stoichiometric base is necessary for formate production, and

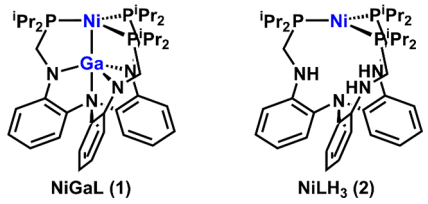

high yields were obtained using Verkade's proazaphosphatrane, 2,8,9-triisopropyl-2,5,8,9-tetraaza-1-phosphabicyclo[3.3.3]-undecane (abbrev. as Vkd).[42,43] Catalyst performance was further optimized by increasing the H_2/CO_2 pressure to 34 atm and decreasing the catalyst loading by 10-fold to 0.03 mol %, which gave near-quantitative generation of formate (Table 1, entries 2 and 3). The corresponding kinetic plot in Figure 2 shows that catalyst **1** attained 3150 formate turnovers in ∼40 min with an initial TOF of 9700 h^{-1}. The high activity of **1** greatly exceeds that of prior Ni homogeneous catalysts (Table S3).[21,23]

A strong base is necessary for catalysis mediated by **1**, as evidenced by trials with bases of varying strengths (pK_a of conjugate acid in CH_3CN): Vkd (33.6),[42] *tert*-butyl tetramethyl guanidine (abbrev. tBuTMG, 26.5),[44] and triethylamine (18.8).[45] Under identical conditions (1 mM **1**, 34 atm 1:1 H_2/CO_2, 293 K), reactions with tBuTMG resulted in a lower yield of formate (80%) and a 30-fold decrease in the maximum rate (Table 1, cf. entries 2 and 4). Moreover, an induction period of ca. 3 h was observed for tBuTMG (Figure 2 inset, SI Figure S9). Of relevance, an initial induction period was also reported for CO_2 hydrogenation catalyzed by $HCo(dmpe)_2$ using a base of comparable strength to tBuTMG.[18,46] With NEt_3, an even weaker base, no formate was generated (entry 5). Presumably, NEt_3 is not sufficiently basic to deprotonate the H_2 adduct, (η^2-H_2)NiGaL, precluding formation of the catalytically active Ni−H species (Figure 1).

The striking effect of the supporting Ga(III) ion is appreciated by comparing **1** with the isostructural Ni-only congener, $NiLH_3$ (**2**).[39,47] No appreciable amount of formate was generated using **2** as the catalyst (entries 6 and 7). Adding $GaCl_3$ as a cocatalyst with **2** also did not yield any formate (entry 8). Altogether, the catalytic results suggest that an intact Ni→Ga interaction (*vide infra*) within our ligand framework provides the requisite tuning effect at Ni to enable catalysis.

Isolating Catalytic Intermediates. Because of the remarkable CO_2 hydrogenation activity by **1** relative to known Ni homogeneous catalysts, we sought to elucidate the role of the supporting Ga(III) ion in promoting catalysis. Previously, the H_2 adduct, (η^2-H_2)NiGaL, was characterized *in situ* using various NMR techniques. In this work, we targeted two later stage intermediates: the Ni(0) anionic hydride and the Ni(0) anionic formate adduct, which is formed after hydride transfer to CO_2 (Figure 1).

The anionic Ni(0) hydride, [VkdH][HNiGaL] ([VkdH]-[**3**]), was generated *in situ* by subjecting a THF-d_8 solution of **1** to 3−5 equiv of Vkd and 1 atm of H_2. The ^{31}P NMR spectrum displayed two new resonances at 76 and −12 ppm in a 3:1 ratio for the ion-paired [HNiGaL]$^-$ and [VkdH]$^+$ fragments, respectively (Figure S10). The single ^{31}P signal of **3** is consistent with retention of C_3 symmetry, while the hydride resonance in the ^{1}H NMR spectrum appears as a broad peak at −6.5 ppm with no discernible coupling even at low temperatures (Figures S11 and S12). Of note, the ^{31}P NMR spectrum of a close analogue, [K(THF)$_x$][**3**], resolves nicely

DOI: 10.1021/jacs.7b07911
J. Am. Chem. Soc. 2017, 139, 14244−14250

Table 1. Catalytic CO_2 Hydrogenation to Formate Using NiGaL (1) or $NiLH_3$ (2) with Various Bases[a]

entry	catalyst	[catalyst] (mM)	base	$P(H_2/CO_2)$ (atm)	theor. TON	actual TON[b]	% yield[c]	TOF (h^{-1}) initial[d]	TOF (h^{-1}) overall[e]
1[f]	**1**	2.9	Vkd	1	275	250	91	67	41
2	**1**	1	Vkd	34	800	800	quant.	3680	2130
3	**1**	0.25	Vkd	34	3200	3150	99	9700	6900
4	**1**	1	tBuTMG	34	800	640	80	120[g]	80
5[h]	**1**	4	NEt_3	34	200	0	0	N.A.	N.A.
6[f]	**2**	2.9	Vkd	1	275	0.8	0.3	0.14[i]	0.04
7	**2**	0.25	Vkd	34	3200	0	0	N.A.	N.A.
8	**2** + $GaCl_3$	0.25	Vkd	34	3200	0	0	N.A.	N.A.

[a]Reaction conditions: catalyst (0.25 to 4 mM), 800 mM base, 1:1 H_2/CO_2 (1 or 34 atm), 0.30 mL of THF-d_8 solution, 293 K. Conditions apply to all entries unless otherwise noted. TON, % yield, and TOF are reported as averages of two trials (see SI Table S2 for details). [b]TON based on ^1H NMR integration of HCO_2^- relative to an internal capillary standard. [c]% yield based on TON/maximum TON, which closely matched ^1H NMR integration of HCO_2^- relative to $H(base)^+$. [d]Initial TOF is the initial slope of the formate turnovers vs time plot (initial ~40 min at 1 atm or 6−10 min at 34 atm). [e]Overall TOF = turnovers/time for >90% of final yield achieved. [f]0.40 mL volume for 1 atm runs. [g]An induction period was observed. Initial TOF defined from ~3.5 to 7.5 h, over which turnovers/time is linear (after induction period). [h]Single run in 0.75 mL of THF in a high-pressure vessel. No HCO_2^- was detected after 150 h at 323 K. [i]Initial TOF determined for the first time point that HCO_2^- was observed (~3 h).

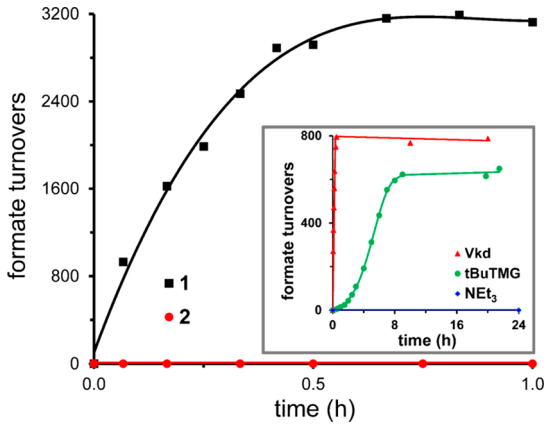

Figure 2. Formate turnovers versus time plots for CO_2 hydrogenation reactions catalyzed by **1** and **2** (0.25 mM catalyst, 800 mM Vkd, 34 atm of 1:1 H_2/CO_2, 293 K, average of two trials for each; see Table 1, entries 3 and 7). Inset shows the kinetic plots for **1** (1 or 4 mM) with various bases (Vkd, tBuTMG, and NEt_3; see Table 1, entries 2, 4, and 5). Full kinetic profiles of all trials are shown in Figures S5−S9.

into a doublet with a $^2J_{P-H}$ of 31.6 Hz (Figure S16). On the basis of the spectroscopic data, we propose that the hydride ligand is terminally bound to the Ni center and resides in the apical pocket *trans* to the Ga(III) ion. In support, density functional theory (DFT) calculations predicted the terminal hydride to be more stable than the bridged Ni(μ-H)Ga isomer (Figure S25, Table S6).

To validate the proposed structure of **3**, the bis(triphenylphosphine)iminium (PPN) analogue was independently prepared and investigated by single-crystal X-ray diffraction. The hydride species was synthesized by adding 1.1 equiv of *n*-BuLi to **1**, presumably via an *in situ* Ni alkyl species that undergoes β-hydride elimination.[26] Subsequent salt exchange with [PPN][tetrakis[3,5-bis(trifluoromethyl)phenyl]borate] ([BArF]$^-$) afforded [PPN][**3**]. Of note, the chemical shifts of the hydride and the phosphines in [PPN][**3**] are nearly identical to those of [VkdH][**3**], implying that [PPN][**3**] is a reasonable model of the catalytically relevant species (Figure S16). From a THF/pentane solution of [PPN][**3**], bright-yellow single crystals were obtained that were suitable for X-ray diffraction. The structural characterization of [PPN][**3**] (Figure 3) is noteworthy because anionic d^{10} hydride complexes are very rare.[48] The only other mononuclear anionic Ni(0) hydride

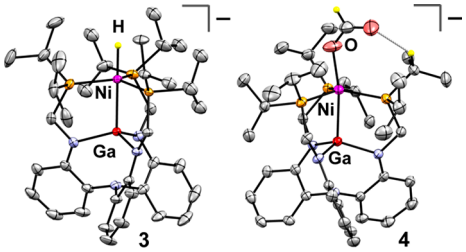

Figure 3. Solid-state structures of [PPN][HNiGaL] ([PPN][**3**], left) and [PPN][(HCO_2)NiGaL] ([PPN][**4**], right) displayed with 50% thermal ellipsoids. The PPN cation and H atoms, except for those on or interacting with the apical ligands, were omitted for clarity. A nonclassical hydrogen-bonding interaction, O(formate)---HC(methine), is shown in **4** (light gray line). Relevant structural parameters of [PPN][**3**] and [PPN][**4**] are shown in Tables S4 and S5.

is [Na(THF)$_4$][HNi(CO)$_3$], which is unstable at room temperature.[49] Moreover, **3** has catalytic utility in that it can be generated from H_2 and base, which is in sharp contrast to the synthesis of [Na(THF)$_4$][HNi(CO)$_3$], where stoichiometric NaHAl(*i*-Bu)$_3$ is employed.

In comparison with NiGaL (**1**), [PPN][**3**] has subtle structural differences that are instructive to consider. One effect of the hydride donor is that the Ni−Ga bond contracts slightly from 2.3789(8) Å in **1** to 2.3549(4) Å in [PPN][**3**] (Figure 3, Table S5).[39] Hence, the dative Ni→Ga interaction remains intact upon the introduction of a *trans* hydride. Perhaps the most informative parameter is the position of the Ni and Ga centers relative to their respective P_3 and N_3 donor sets. In [PPN][**3**], both Ni and Ga are displaced further above the P_3- and N_3-planes by 0.07 and 0.17 Å, respectively, than in **1**. Intriguingly, the displacement of Ga is more than double that of Ni upon introduction of the hydride ligand despite the fact that the hydride only interacts directly with Ni. This striking structural feature underscores the cooperativity of the Ni−Ga unit, as both metals reposition to accommodate the incoming hydride ligand. A complementary interpretation is that a strong

DOI: 10.1021/jacs.7b07911
J. Am. Chem. Soc. 2017, 139, 14244−14250

Ni→Ga dative interaction assists in stabilizing the electron-rich, anionic Ni−H moiety.

Next, we sought to characterize the anionic Ni formate intermediate $[(HCO_2)NiGaL]^-$ (**4**), which appears in the catalytic cycle following hydride transfer to CO_2 (Figure 1). The formate species [VkdH][**4**] was generated *in situ* by exposure of [VkdH][**3**] to CO_2 (1 atm) or by addition of excess (∼4 equiv) $[VkdH][HCO_2]$ to **1**. A diagnostic ^{1}H NMR resonance at 8.68 ppm is assigned to the proton of the coordinated formate (cf. 8.79 ppm for free [VkdH][formate],[46] Figure S20). This intermediate was also isolated as the PPN ion-pair by exposing [PPN][**3**] to CO_2. The solid-state structure of the resulting complex, $[PPN][(HCO_2)NiGaL]$ ([PPN][**4**]), shows an η^1-*O* formate ligand and an intact Ni−Ga bond of 2.3789(5) Å, which is essentially identical to that of **1** (Figure 3, Table S5).

Understanding the Ni(0) Hydride Intermediate (3). To gain additional insight into the nature of the Ni(0)−H bond, we undertook a complementary experimental and theoretical investigation of $[HNiGaL]^-$. By IR spectroscopy, a KBr pellet of [PPN][**3**] displayed a broad band of medium intensity at 1696 cm^{-1}, which shifted to 1226 cm^{-1} upon deuteration (Figure S26). The Ni−H vibrational frequency was further confirmed by a closely matched value of 1697 cm^{-1} from DFT calculations (Figure S27). Of note, this frequency value is extremely low for terminal hydrides of Ni and nearly ties with CpNi(IMes)H (1695 cm^{-1}) for the lowest Ni−H stretching frequency.[26,50]

Another useful parameter for comparing the reactivity of metal hydride complexes is the thermodynamic hydricity ($\Delta G^\circ_{H^-}$), or the free energy needed to cleave a M−H bond to generate a hydride ion.[41,51] The $\Delta G^\circ_{H^-}$ of $[HNiGaL]^-$ was experimentally determined by measuring the H_2 heterolysis equilibrium with NiGaL and Vkd base (eq 1), in conjunction with the known pK_a of $VkdH^+$ (eq 2) and the H_2 heterolysis constant (known in CH_3CN, eq 3), as shown below.[27,41]

$$[HNiGaL]^- + VkdH^+ \rightleftharpoons NiGaL + H_2 + Vkd \qquad \Delta G^\circ_1 = -RT\ln(K_{eq}) \tag{1}$$

$$Vkd + H^+ \rightleftharpoons VkdH^+ \qquad \Delta G^\circ_2 = -1.364(pK_a) \tag{2}$$

$$H_2 \rightleftharpoons H^+ + H^- \qquad \Delta G^\circ_3 = +76\ \text{kcal/mol} \tag{3}$$

net:

$$[HNiGaL]^- \rightleftharpoons NiGaL + H^- \qquad \Delta G^\circ_{H^-} = \Delta G^\circ_1 + \Delta G^\circ_2 + \Delta G^\circ_3$$

Hydricity values are typically measured in CH_3CN since ΔG°_3 is known (eq 3), and so one caveat to estimating the absolute hydricity of $[HNiGaL]^-$ is that K_{eq} of eq 1 was measured in THF due to complications arising from poor solubility of NiGaL in CH_3CN and competitive binding between H_2 and CH_3CN (see SI). K_{eq} of eq 1 was measured to be 0.16 in THF based on two independent trials employing different base concentrations (Figures S30−S32, Tables S8−S9). If K_{eq} of eq 1 is comparable in THF and CH_3CN solvents, one can estimate $\Delta G^\circ_{H^-} \approx 31.3(5)$ kcal/mol for $[HNiGaL]^-$ in CH_3CN. Alternatively, one can rigorously measure the difference in $\Delta G^\circ_{H^-}$ values between $[HNiGaL]^-$ and H_2 in THF, or $\Delta G^\circ_{H^-}(\mathbf{3}) - \Delta G^\circ_{H^-}(H_2)$, is −37.1(6) kcal/mol in THF and, of interest, is comparable to $\Delta G^\circ_{H^-}(\mathbf{3}) - \Delta G^\circ_{H^-}(H_2)$ in CH_3CN of −45 kcal/mol, using the *estimated* $\Delta G^\circ_{H^-}(\mathbf{3})$ of 31 kcal/mol.

To further test the assumption that measuring K_{eq} of eq 1 in THF can lead to meaningful comparisons with $\Delta G^\circ_{H^-}$ values obtained wholly in CH_3CN, we probed the hydride transfer equilibrium between **1** and $HCo(dmpe)_2$ (known $\Delta G^\circ_{H^-} = 36$ kcal/mol in CH_3CN).[18] No hydride transfer to NiGaL was detected in THF over 2.5 weeks, suggesting that the $\Delta G^\circ_{H^-}$ value of $[HNiGaL]^-$ is <33 kcal/mol (Figure S33). In the reverse direction, essentially full consumption of $[HNiGaL]^-$ and $[Co(dmpe)_2]^+$ to give $(CH_3CN)NiGaL$ and $HCo(dmpe)_2$ was observed within 3 days in ∼3:1 CH_3CN/THF, confirming that the lack of hydride transfer between $HCo(dmpe)_2$ and NiGaL was due to the greater thermodynamic stability of $HCo(dmpe)_2$ relative to $[HNiGaL]^-$ rather than sluggish hydride transfer kinetics (Figure S33). Additionally, DFT studies of isodesmic hydride transfer between $[HNiGaL]^-$ and $[Ni(dmpe)_2]^{2+}$ in CH_3CN predicted a hydricity of 28−31 kcal/mol for $[HNiGaL]^-$, which matches the experimental estimate (Table S11).[34] The importance of Ga(III) for stabilizing the anionic Ni−H is, perhaps, underscored by our inability to synthetically generate the $[H{-}NiLH_3]^-$ analogue. We also note that we have not observed H_2 binding to $NiLH_3$ even at high pressure and low temperature (34 atm H_2, 193 K), nor have we observed H_2 deprotonation to give a $[H{-}NiLH_3]^-$ analogue using excess strong base (Vkd base or potassium *tert*-butoxide).

For comparison, $[HNi(diphosphine)_2]^+$ complexes have hydricity values that range from 50 to 68 kcal/mol.[41] With a considerably lower $\Delta G^\circ_{H^-}$ value (31 kcal/mol), $[HNiGaL]^-$ is, by a wide margin, the strongest hydride donor of any Ni−H reported to date. The exceptional hydricity of $[HNiGaL]^-$ can be attributed to its anionic charge and the zerovalent oxidation state of Ni, which is distinct from the cationic Ni(II) hydrides in the literature.[26] Notably, $[HNiGaL]^-$ is among the strongest hydride donors of any first-row metal complex (cf. $HCo(P_4N_2)$, $\Delta G^\circ_{H^-} = 31.8$ kcal/mol)[52] and is even on par with some of the more hydridic precious metal complexes, (e.g., HRh(diphosphine)$_2$, $\Delta G^\circ_{H^-} = 26{-}34$ kcal/mol).[41] Of relevance to catalysis, the low $\Delta G^\circ_{H^-}$ of $[HNiGaL]^-$ would allow for direct outer-sphere hydride transfer to CO_2 with a driving force of ∼13 kcal/mol.[28] It should be noted, however, that the driving force in catalysis is likely greater for the conversion of [VkdH][**3**] and CO_2 to [VkdH][**4**] due to enthalpic contributions from subsequent Ni−O bond formation in the formate adduct after initial hydride transfer (*vide infra*).

Perhaps, the most unexpected feature of **3** is its stability as an anionic d^{10} hydride.[48] A simple bonding analysis between a d^{10} metal and H^- would require the M−H σ-antibonding orbital to be fully populated. Natural orbitals obtained from complete active space self-consistent field (CASSCF)[53] calculations, however, revealed a distinctly different bonding scheme. While the five Ni 3d orbitals are indeed doubly occupied, consistent with Ni(0), they show essentially no bonding to the hydride. Rather, the natural orbital involved in Ni−H σ-bonding has both metal contributions [29% Ni, primarily 4p$_z$; 10% Ga, 4s/4p$_z$] and substantial hydridic character [51% H(1s)] (Figure 4, Table S13).

We further propose that the Ni→Ga interaction is critical for stabilizing the Ni(0)−H bond because of the symbiotic nature of two σ-bonding interactions: (1) donation of hydride to Ni, via H(1s)→Ni(4p$_z$/4s) and (2) donation from Ni to Ga, via

DOI: 10.1021/jacs.7b07911
J. Am. Chem. Soc. 2017, 139, 14244−14250

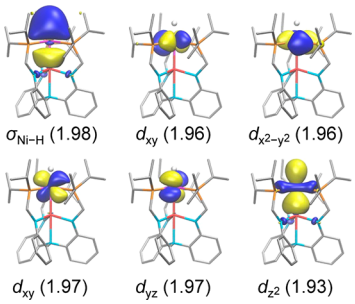

Figure 4. Selected natural orbitals obtained from a CASSCF calculation of [HNiGaL]$^-$ (**3**). Occupation numbers (shown in parentheses) indicate that these six orbitals are doubly occupied. Refer to Figure S34 and Table S13 for additional details.

Ni($3d_{z2}$)→Ga($4p_z$/4s). This stabilization of the Ni(0)−H by Ga(III) can be interpreted as an *inverse trans influence* exerted by the Ga metalloligand,[54] which acts as a σ-acceptor[55,56] toward Ni and strengthens the Ni−H bond directly *trans* to it ("pull−pull"). In support, a natural bond orbital analysis shows that the Ni→Ga stabilization energy increases by 10 kcal/mol from NiGaL (**1**) to [HNiGaL]$^-$ (**3**) (Figure S35, Table S14).[57]

Mechanistic Insights. A simple catalytic cycle is proposed (Figure 1): (1) H_2 binding to NiGaL forms (η^2-H_2)NiGaL, (2) deprotonation by base generates [HNiGaL]$^-$, (3) hydride transfer to CO_2 forms [(η^1-HCO_2)NiGaL]$^-$, and (4) liberation of formate regenerates NiGaL. This catalytic mechanism is commonly proposed, albeit typically with $M(H)_2^+$ and a neutral M−H as the catalytic intermediates instead of the M(η^2-H_2) and anionic M−H species proposed here.[3]

The feasibility of the proposed mechanism is further demonstrated by complementary reactivity studies. Initial binding of H_2 is favored, as **1** showed no propensity to bind CO_2 even under 34 atm. Deprotonation of (η^2-H_2)NiGaL to generate [HNiGaL]$^-$ occurred readily in the presence of H_2 (1 atm) and excess Vkd (Figures S10 and S11). Of interest, the pK_a^{THF} of (η^2-H_2)NiGaL was measured to be 27.5(2) via the proton transfer equilibrium between (η^2-H_2)NiGaL and Vkd in the overall H_2 heterolysis reaction (eq 1, Table S9). This supports the hypothesis that a strong base is necessary to form the active species, [HNiGaL]$^-$. For comparison, the pK_a^{THF} of H_2 is estimated to be 49,[58] which means that the acidity of H_2 increases by 21 pK_a units upon binding to NiGaL. This drastic increase in the acidity of H_2 upon binding to Ni, which allows for deprotonation to give the catalytically relevant anionic hydride, is not observed for $NiLH_3$, rendering it essentially catalytically inactive (*vide supra*). Finally, the reaction between [VkdH][HNiGaL] and CO_2 (1 atm) was observed to form [VkdH][(HCO_2)NiGaL] (Figure S22). Additionally, isotopic labeling studies confirmed that formate was derived from D_2 and $^{13}CO_2$ (Figure S38).

Monitoring the Ni speciation during catalysis also provided unique insights. Throughout catalysis, the observed catalyst resting state is the formate species [VkdH][**4**] (Figure S36). From [VkdH][**4**], regeneration of the catalytically active [VkdH][**3**] was observed to occur upon the addition of H_2 (1 atm) in the presence of Vkd (Figure S37). The buildup of the formate complex during catalysis suggests the rate-limiting step is the liberation of [VkdH][HCO_2] to regenerate NiGaL. In highly active Fe and Co pincer systems with TONs of ∼10^4, formate dissociation is also sluggish, and Li^+ additives (0.1 to 0.2 equiv per base) are needed to promote formate loss and drive catalytic turnover.[19,20] In the present system, no additives were used. Presumably, formate extrusion is enhanced by the overall anionic charge of the Ni formate intermediate and the weaker Ni(0)−OCHO bond.

■ CONCLUSION

In summary, we have shown that a Lewis acidic Ga(III) supporting ion can interact with Ni to enable direct CO_2 hydrogenation to formate at ambient temperature with excellent yields. The high formate turnovers (3150) and TOF (9700 h^{-1}) are unprecedented for Ni and respectable compared to state-of-the-art homogeneous first-row metal catalysts (i.e., Fe, Co). The Ga(III) support plays a pivotal role in stabilizing the unusual anionic [HNiGaL]$^-$ species, which is by far the strongest hydride donor reported to date for Ni ($\Delta G^\circ_{H^-} \approx 31$ kcal/mol) and is on par with the most hydridic first-row and many precious metal hydrides. The significance of the Lewis acidic Ga(III) support is further emphasized via comparison to $NiLH_3$, which is essentially inactive for CO_2 hydrogenation due to its inability to bind and activate H_2 toward deprotonation to stabilize an analogous anionic hydride. Future studies will further elucidate the catalytic mechanism and detail the roles of the Ga(III) supporting ion therein, as well as investigate the influence of other group 13 Lewis acidic supports on Ni-catalyzed CO_2 hydrogenation.

■ EXPERIMENTAL SECTION

High-Pressure Catalytic Reactions. CO_2 hydrogenation reactions at 34 atm of ∼1:1 H_2/CO_2 were performed in PEEK high-pressure NMR spectroscopy tubes designed and built at Pacific Northwest National Laboratory, as reported previously.[59] In a typical catalytic experiment (0.25 mM NiGaL (**1**), 800 mM Vkd base), a stock solution of **1** (11.8 mg, 14.6 μmol) in 1 mL of THF-d_8 was prepared. A 0.875 M solution of Vkd (168 mg, 560 μmol) in 640 μL of THF-d_8 was also prepared. From these stock solutions, a catalyst mixture stock solution was prepared (700 μL of 800 mM Vkd, 0.25 mM NiGaL). Note that preparations were adjusted accordingly to afford other concentrations of NiGaL (or $NiLH_3$) and/or other bases, including tBuTMG and NEt_3. Lastly, 300 μL of the reaction solution was added to two different PEEK NMR spectroscopy cells.

The PEEK cell was sealed and connected to a purged high-pressure line equipped with a vacuum pump and an ISCO syringe pump. The headspace was degassed by opening the PEEK cell to static vacuum (3 × 10 s). Gas was delivered to the cell from an ISCO syringe pump running constantly at 34 atm (i.e., continuous gas feed). The contents of the PEEK cells were mixed using a vortex mixer for approximately 3 min until the pressure stabilized. After stabilization, the cell was inserted into the NMR spectrometer periodically to acquire data over time. The contents of the PEEK cell were mixed using a vortex mixer when NMR spectra were not being collected to promote optimal gas−liquid mixing throughout catalysis. The concentration of formate was determined by integrating the formate resonance relative to the residual HDO resonance in the $CoCl_2$ in D_2O capillary standard.

Synthesis of [N(P(C_6H_5)$_3$)$_2$][HNiGa(N(*o*-($NCH_2P^iPr_2$)C_6H_4)$_3$)] (abbrev. as [PPN][3]). A stirring solution of NiGaL (114 mg, 138 μmol) in 8 mL of THF was cooled to −78 °C over 15 min. To this solution was added 62.5 μL (156 μmol) of *n*-BuLi solution (2.5 M in hexanes), and the color rapidly changed from deep-red to red-yellow. This solution was allowed to warm to room temperature over the course of 12 h. Subsequent salt exchange was performed by adding solid bis(triphenylphosphine)iminium tetrakis[3,5-bis-(trifluoromethyl)phenyl]borate ([PPN][$BArF_{24}$], 415 mg, 283 μmol), and the solution was concentrated *in vacuo*, resulting in the precipitation of solids. Et_2O was added until the total volume was ∼20 mL, and the mixture was stirred vigorously for 3 h, affording a bright yellow precipitate. This precipitate was washed with Et_2O (2 × 10 mL) to give [PPN][**3**] as a bright-yellow powder (101 mg, 731 μmol, 40%

DOI: 10.1021/jacs.7b07911
J. Am. Chem. Soc. 2017, 139, 14244−14250

yield). Single crystals of [PPN][**3**] suitable for X-ray diffraction were grown by layering a THF solution with pentane. Additionally, the analogous deuteride complex [PPN][**3**(D)] was synthesized *in situ* by overnight exposure of [PPN][**3**] (10 mg, 7.4 μmol) to D_2 (4 atm) in THF-d_8 in a J. Young NMR tube.

$^1H\{^{31}P\}$ NMR (ppm, THF-d_8, 400 MHz): 7.62 (t, J = 7.4 Hz, PPN, 6H), 7.56 (d, J = 7.7 Hz, PPN, 12H), 7.44 (t, J = 7.5 Hz, PPN, 12H), 7.12 (d, J = 7.4 Hz, aryl, 3H), 6.56 (t, J = 7.5 Hz, aryl, 3H), 6.14 (d, J = 7.9 Hz, aryl, 3H), 5.94 (t, J = 7.3 Hz, aryl, 3H), 2.60 (br, $CH_2P(^iPr)_2$, 6H), 1.77 (br, $CH(CH_3)_2$, 3H), 1.56 (br, $C'H(CH_3)_2$, 3H), 1.05−0.60 (br, $CH(CH_3)_2$, 36H), −6.45 (br, NiH, 1H, T_1(min) ≤ 0.84(4) s at 233 K). $^{31}P\{^1H\}$ NMR (ppm, THF-d_8, 162 MHz): 75.3 (s, 3P, HNiGaL$^-$), 21.0 (s, 2P, PPN). IR (KBr pellet, cm^{-1}): ν(Ni−H) 1696 [1226 for **3**(D)]. Anal. Calcd for [PPN][**3**], [$C_{36}H_{30}NP_2$]-[$C_{39}H_{61}N_4P_3NiGa$] (%): C, 66.93; H, 6.82; N, 5.20. Anal. Calcd for [PPN][**3**·O_2] (%): C, 65.38; H, 6.66; N, 5.08. Found: C, 65.24; H, 6.90; N, 4.86. Elemental analysis consistently showed a low carbon percentage that could be consistent with oxidation by one equivalent of O_2.

Computational Methods. Density functional theory and *ab initio* wave function calculations were performed for anionic complexes **3** and **4**. Geometries were fully optimized in the gas phase using Gaussian 09 software[60] and the M06-L[61] local functional with def2-series basis sets,[62] denoted as M06-L/DEF2 (see SI for details). Vibrational frequency calculations were performed to confirm the stationary point nature of the structures. Solvation effects were considered by performing single-point calculations for all stationary points using the SMD solvation model with either THF or CH_3CN as the solvent.[63] Isodesmic hydride transfer reactions were modeled by DFT using several different functionals to benchmark the hydricity of **3** relative to those of other previously reported M−H (see Tables S10 and S11).[34] Complex **3** was further investigated by *ab initio* calculations using the CASSCF[53] method. CASSCF calculations were performed on the M06-L/DEF2-optimized structures using the MOLCAS-8.1 package[64] with relativistic basis sets of atomic natural orbitals types; that is, ANO-RCC-VDZ[65] were used for N, P, C, and H atoms and ANO-RCC-VTZ were used for Ni and Ga atoms. The Ni→Ga dative bond was also interrogated by calculating the donor−acceptor stabilization energies for **3** (in comparison to **1**) based on natural bond orbital analysis.[57]

■ ASSOCIATED CONTENT

Supporting Information

The Supporting Information is available free of charge on the ACS Publications website at DOI: 10.1021/jacs.7b07911.

Crystallographic data for [PPN][**3**] (CIF)
Crystallographic data for [PPN][**4**] (CIF)
Additional data for catalysis studies, synthesis of **4**, spectroscopic characterization, computational studies, and hydricity measurements; XYZ files for DFT-optimized geometries (PDF)

■ AUTHOR INFORMATION

Corresponding Author

*clu@umn.edu

ORCID

Jing Xie: 0000-0001-9676-5734
Jingyun Ye: 0000-0003-4373-9625
John C. Linehan: 0000-0001-8942-7163
Aaron M. Appel: 0000-0002-5604-1253
Laura Gagliardi: 0000-0001-5227-1396
Connie C. Lu: 0000-0002-5162-9250

Notes

The authors declare no competing financial interest.

These cif files for [PPN][**3**] and [PPN][**4**] have been deposited in the Cambridge CCDC as nos. 1553935−1553936.

■ ACKNOWLEDGMENTS

R.C.C. and M.V.V. were supported by DOE Office of Science Graduate Student Research and National Science Foundation (NSF) Graduate Research Fellowship programs, respectively. J.X., J.Y., and L.G. were supported as part of the Inorganometallic Catalyst Design Center, an Energy Frontier Research Center funded by the U.S. Department of Energy (DOE), Office of Science, Basic Energy Sciences under Award DE-SC0012702. J.C.L., S.A.B., and A.M.A. were supported by the U.S. Department of Energy, Office of Science, Office of Basic Energy Sciences, Division of Chemical Sciences, Geosciences & Biosciences. C.C.L. acknowledges the NSF (CHE-1665010) for support. The authors acknowledge Dr. Victor Young, Jr. for assistance with X-ray crystallography. R.C.C. thanks Dr. Christopher Zall and Dr. Eric Wiedner for helpful suggestions. C.C.L. thanks Dr. Morris Bullock (PNNL) for co-sponsoring the DOE graduate research fellowship to R.C.C.

■ REFERENCES

(1) Olah, G. A.; Prakash, G. K. S.; Goeppert, A. *J. Am. Chem. Soc.* **2011**, *133*, 12881−12898.
(2) Appel, A. M.; Bercaw, J. E.; Bocarsly, A. B.; Dobbek, H.; DuBois, D. L.; Dupuis, M.; Ferry, J. G.; Fujita, E.; Hille, R.; Kenis, P. J. A.; Kerfeld, C. A.; Morris, R. H.; Peden, C. H. F.; Portis, A. R.; Ragsdale, S. W.; Rauchfuss, T. B.; Reek, J. N. H.; Seefeldt, L. C.; Thauer, R. K.; Waldrop, G. L. *Chem. Rev.* **2013**, *113*, 6621−6658.
(3) Wang, W.-H.; Himeda, Y.; Muckerman, J. T.; Manbeck, G. F.; Fujita, E. *Chem. Rev.* **2015**, *115*, 12936−12973.
(4) Klankermayer, J.; Wesselbaum, S.; Beydoun, K.; Leitner, W. *Angew. Chem., Int. Ed.* **2016**, *55*, 7296−7343.
(5) Aresta, M.; Dibenedetto, A. *Dalton Trans.* **2007**, 2975−2992.
(6) Wesselbaum, S.; vom Stein, T.; Klankermayer, J.; Leitner, W. *Angew. Chem., Int. Ed.* **2012**, *51*, 7499−7502.
(7) Wesselbaum, S.; Moha, V.; Meuresch, M.; Brosinski, S.; Thenert, K. M.; Kothe, J.; von Stein, T.; Englert, U.; Hölscher, M.; Klankermayer, J.; Leitner, W. *Chem. Sci.* **2015**, *6*, 693−704.
(8) Huff, C. A.; Sanford, M. S. *J. Am. Chem. Soc.* **2011**, *133*, 18122−18125.
(9) Kothandaraman, J.; Goeppert, A.; Czaun, M.; Olah, G. A.; Prakash, G. K. S. *J. Am. Chem. Soc.* **2016**, *138*, 778−781.
(10) Rezayee, N. M.; Huff, C. A.; Sanford, M. S. *J. Am. Chem. Soc.* **2015**, *137*, 1028−1031.
(11) Sordakis, K.; Tsurusaki, A.; Iguchi, M.; Kawanami, H.; Himeda, Y.; Laurenczy, G. *Chem. - Eur. J.* **2016**, *22*, 15605−15608.
(12) Schneidewind, J.; Adam, R.; Baumann, W.; Jackstell, R.; Beller, M. *Angew. Chem., Int. Ed.* **2017**, *56*, 1890−1893.
(13) Federsel, C.; Boddien, A.; Jackstell, R.; Jennerjahn, R.; Dyson, P. J.; Scopelliti, R.; Laurenczy, G.; Beller, M. *Angew. Chem., Int. Ed.* **2010**, *49*, 9777−9780.
(14) Langer, R.; Diskin-Posner, Y.; Leitus, G.; Shimon, L. J. W.; Ben-David, Y.; Milstein, D. *Angew. Chem., Int. Ed.* **2011**, *50*, 9948−9952.
(15) Ziebart, C.; Federsel, C.; Anbarasan, P.; Jackstell, R.; Baumann, W.; Spannenberg, A.; Beller, M. *J. Am. Chem. Soc.* **2012**, *134*, 20701−20704.
(16) Federsel, C.; Ziebart, C.; Jackstell, R.; Baumann, W.; Beller, M. *Chem. - Eur. J.* **2012**, *18*, 72−75.
(17) Zell, T.; Milstein, D. *Acc. Chem. Res.* **2015**, *48*, 1979−1994.
(18) Jeletic, M. S.; Mock, M. T.; Appel, A. M.; Linehan, J. C. *J. Am. Chem. Soc.* **2013**, *135*, 11533−11536.
(19) Zhang, Y.; MacIntosh, A. D.; Wong, J. L.; Bielinski, E. A.; Williard, P. G.; Mercado, B. Q.; Hazari, N.; Bernskoetter, W. H. *Chem. Sci.* **2015**, *6*, 4291−4299.
(20) Spentzos, A. Z.; Barnes, C. L.; Bernskoetter, W. H. *Inorg. Chem.* **2016**, *55*, 8225−8233.

DOI: 10.1021/jacs.7b07911
J. Am. Chem. Soc. 2017, 139, 14244−14250

(21) Inoue, Y.; Izumida, H.; Sasaki, Y.; Hashimoto, H. *Chem. Lett.* **1976**, *5*, 863−864.
(22) Tai, C.-C.; Chang, T.; Roller, B.; Jessop, P. G. *Inorg. Chem.* **2003**, *42*, 7340−7341.
(23) Burgess, S. A.; Kendall, A. J.; Tyler, D. R.; Linehan, J. C.; Appel, A. M. *ACS Catal.* **2017**, *7*, 3089−3096.
(24) Enthaler, S.; Brück, A.; Kammer, A.; Junge, H.; Irran, E.; Gülak, S. *ChemCatChem* **2015**, *7*, 65−69.
(25) Harman, W. H.; Peters, J. C. *J. Am. Chem. Soc.* **2012**, *134*, 5080−5082.
(26) Eberhardt, N. A.; Guan, H. *Chem. Rev.* **2016**, *116*, 8373−8426.
(27) Curtis, C. J.; Miedaner, A.; Ellis, W. W.; DuBois, D. L. *J. Am. Chem. Soc.* **2002**, *124*, 1918−1925. The hydricity value for $[HNi(dmpe)_2]^+$ has since been updated to 49.9 kcal/mol using more recently developed self-consistent pK_a scales (ref 41).
(28) DuBois, D. L.; Berning, D. E. *Appl. Organomet. Chem.* **2000**, *14*, 860−862.
(29) Chakraborty, S.; Zhang, J.; Krause, J. A.; Guan, H. *J. Am. Chem. Soc.* **2010**, *132*, 8872−8873.
(30) A Ni dicarbene catalyst: Lu, Z.; Williams, T. J. *ACS Catal.* **2016**, *6*, 6670−6673.
(31) Zimmermann, P.; Limberg, C. *J. Am. Chem. Soc.* **2017**, *139*, 4233−4242.
(32) Yoo, C.; Lee, Y. *Angew. Chem., Int. Ed.* **2017**, *56*, 9502−9506.
(33) Mondal, B.; Neese, F.; Ye, S. *Inorg. Chem.* **2016**, *55*, 5438−5444.
(34) Qi, X.-J.; Fu, Y.; Liu, L.; Guo, Q.-X. *Organometallics* **2007**, *26*, 4197−4203.
(35) Rudd, P. A.; Liu, S.; Gagliardi, L.; Young, V. G.; Lu, C. C. *J. Am. Chem. Soc.* **2011**, *133*, 20724−20727.
(36) Bouhadir, G.; Bourissou, D. *Chem. Soc. Rev.* **2016**, *45*, 1065−1079 and references therein. See refs 37 and 38 for recent examples of bifunctional catalysts with a sigma acceptor ligand at the metal.
(37) Takaya, J.; Iwasawa, N. *J. Am. Chem. Soc.* **2017**, *139*, 6074−6077.
(38) You, D.; Gabbaï, F. P. *J. Am. Chem. Soc.* **2017**, *139*, 6843−6846.
(39) Cammarota, R. C.; Lu, C. C. *J. Am. Chem. Soc.* **2015**, *137*, 12486−12489.
(40) Cammarota, R. C.; Clouston, L. J.; Lu, C. C. *Coord. Chem. Rev.* **2017**, *334*, 100−111.
(41) Wiedner, E. S.; Chambers, M. B.; Pitman, C. L.; Bullock, R. M.; Miller, A. J. M.; Appel, A. M. *Chem. Rev.* **2016**, *116*, 8655−8692.
(42) Kisanga, P. B.; Verkade, J. G.; Schwesinger, R. *J. Org. Chem.* **2000**, *65*, 5431−5432.
(43) Wróblewski, A. E.; Pinkas, J.; Verkade, J. G. *Main Group Chem.* **1995**, *1*, 69−79.
(44) Zall, C. M.; Linehan, J. C.; Appel, A. M. *ACS Catal.* **2015**, *5*, 5301−5305.
(45) Kaljurand, I.; Kütt, A.; Sooväli, L.; Rodima, T.; Mäemets, V.; Leito, I.; Koppel, I. A. *J. Org. Chem.* **2005**, *70*, 1019−1028.
(46) Jeletic, M. S.; Helm, M. L.; Hulley, E. B.; Mock, M. T.; Appel, A. M.; Linehan, J. C. *ACS Catal.* **2014**, *4*, 3755−3762.
(47) Clouston, L. J.; Siedschlag, R. B.; Rudd, P. A.; Planas, N.; Hu, S.; Miller, A. D.; Gagliardi, L.; Lu, C. C. *J. Am. Chem. Soc.* **2013**, *135*, 13142−13148.
(48) Darensbourg, M. Y.; Ash, C. E. In *Advances in Organometallic Chemistry*; Stone, F. G. A., West, R., Eds.; Academic Press, Inc.: San Diego, CA, 1987.
(49) Kleimann, W.; Pörschke, K.-R.; Wilke, G. *Chem. Ber.* **1985**, *118*, 323−331.
(50) Abernethy, C. D.; Baker, R. J.; Cole, M. L.; Davies, A. J.; Jones, C. *Transition Met. Chem.* **2003**, *28*, 296−299.
(51) Berning, D. E.; Noll, B. C.; DuBois, D. L. *J. Am. Chem. Soc.* **1999**, *121*, 11432−11447.
(52) Wiedner, E. S.; Appel, A. M.; DuBois, D. L.; Bullock, R. M. *Inorg. Chem.* **2013**, *52*, 14391−14403.
(53) Roos, B. O.; Taylor, P. R.; Siegbahn, P. E. M. *Chem. Phys.* **1980**, *48*, 157−173.
(54) Vollmer, M. V.; Xie, J.; Lu, C. C. *J. Am. Chem. Soc.* **2017**, *139*, 6570−6573.
(55) Parkin, G. *Organometallics* **2006**, *25*, 4744−4747.
(56) Amgoune, A.; Bourissou, D. *Chem. Commun.* **2011**, *47*, 859−871.
(57) Weinhold, F.; Landis, C. R. *Chem. Educ. Res. Pract.* **2001**, *2*, 91−104.
(58) Abdur-Rashid, K.; Fong, T. P.; Greaves, B.; Gusev, D. G.; Hinman, J. G.; Landau, S. E.; Lough, A. J.; Morris, R. H. *J. Am. Chem. Soc.* **2000**, *122*, 9155−9171.
(59) Yonker, C. R.; Linehan, J. C. *J. Organomet. Chem.* **2002**, *650*, 249−257.
(60) Frisch, M.; Trucks, G.; Schlegel, H.; Scuseria, G.; Robb, M.; Cheeseman, J.; Scalmani, G.; Barone, V.; Mennucci, B.; Petersson, G. *Gaussian 09*, revision D. 01; Gaussian, Inc.: Wallingford, CT, 2009.
(61) Zhao, Y.; Truhlar, D. G. *J. Chem. Phys.* **2006**, *125*, 194101.
(62) Weigend, F.; Ahlrichs, R. *Phys. Chem. Chem. Phys.* **2005**, *7*, 3297−3305.
(63) Marenich, A. V.; Cramer, C. J.; Truhlar, D. G. *J. Phys. Chem. B* **2009**, *113*, 6378−6396.
(64) Aquilante, F.; Autschbach, J.; Carlson, R. K.; Chibotaru, L. F.; Delcey, M. G.; De Vico, L.; Ferré, N.; Frutos, L. M.; Gagliardi, L.; Garavelli, M. *J. Comput. Chem.* **2016**, *37*, 506−541.
(65) Roos, B. O.; Lindh, R.; Malmqvist, P.-Å.; Veryazov, V.; Widmark, P.-O. *J. Phys. Chem. A* **2004**, *108*, 2851−2858.

DOI: 10.1021/jacs.7b07911
J. Am. Chem. Soc. 2017, 139, 14244−14250